

# Reflectance Estimation of Outdoor Diffuse Object with the Presence of Interreflection

Hongxun Zhao, Sonoko Okura, Rei Kawakami, Katsushi Ikeuchi

Institute of Industrial Science, The University of Tokyo

**Abstract** It is necessary to acquire the accurate reflectance properties of an object, if we want to use this object as a model for computer vision and graphics applications. However, wrong reflectance parameters are estimated, when interreflection exists. Interreflections are negligible for convex objects, while it is not for concave objects. This paper addresses a method to estimate diffuse reflectance parameters of an outdoor object with the presence of interreflection. This paper solve the problem by assuming that a surface consists of hundreds of small facets. The interreflection effect on a facet is calculated as the sum of incoming light energy from all the other facets. Experimental evaluation on both simulation and real outdoor objects shows the improvement achieved by this method.

## 1 Introduction

In order to make a realistic object model for computer graphics applications, shape and optical information of the object are necessary. As a result of significant advancement of range sensors and data processing algorithms, shape of an object becomes acquirable without much difficulties [1] [2]. However, obtaining the optical information of the object remains a challenge, because the reflectance properties of a real object are usually very complicated.

One reason of this complexity is the interreflection between object surfaces. Light rays that we observe is the result of reflections repeated between surfaces infinitely. It is difficult to trace back those recursive reflections from the observation, and therefore, only few works that handle interreflection with regards to reflectance estimation have proposed.

The early work has been done by Nayar et al. [3]. They estimated the shape and surface reflectance of a concave object, which has a lot of interreflections inside. In the method, the object is assumed to have a uniform surface reflectance. Another inverse-global-illumination method is proposed by Yu and Debevec [4]. The method is applied for an indoor room, and it requires images from different view points to cover the whole room. The light positions have to be known in the method.

In this paper, we propose a method to estimate the reflectance of an outdoor object with the presence of interreflection which based on the technique addressed by Nayar et al. [3]. Assuming that a surface consists of hundreds of small facets, the interreflection effect on one facet is calculated as the sum of incoming light energy from all the other facets.

This paper is organized as follows: Section 2 describes how to calculate radiance and irradiance values of the object surface. Section 3 explains our method for estimating the surface reflectance of the object with the presence of interreflection. Section 4 shows the experimental results

for both simulation and real outdoor object. Conclusion are summarized in Section 5. Appendix describes the definition of radiance and irradiance used in this paper.

### 1.1 Related Work

In the early years, textures of an object were modeled by linearly combining multiple reference textures [5] [6] [7] [8] [9]. In order to create more realistic and physically correct model of an object, a lot of methods have been proposed in the last two decades, such as physics-based reflectance parameter estimations [10] [11] [12], and image-based renderings [13] [14].

Sato and Ikeuchi [15] proposed a method to estimate reflectance properties by taking a number of images under varying illumination conditions. The method estimates accurate reflectance of both diffuse and specular components. Nayar et al. [16] developed a technique to separate the direct and global components of a scene using high frequency illumination. The direct component means the brightness of a scene whose radiance value is directly due to the light source, while the global component represents radiance value due to the other points in the scene. By projecting two complement patterns to illuminate the objects, the direct and global components can be separated. Those methods are only applicable for indoor objects.

Weiss [17] proposed a method to separate the illumination and reflectance of an outdoor scene by using the derivate filter. The method requires a sequence of images of a whole day, and does not take the interreflection into account.

## 2 Radiance and Irradiance Values of Object Surface

In general, when assuming the object surface is Lambertian and there is no interreflection, the reflectance of an object can be derived from the bidirectional reflectance distribution function  $f = \frac{L}{E}$ , where  $L$  and  $E$  are the radiance and irradiance values of object surface, respectively.

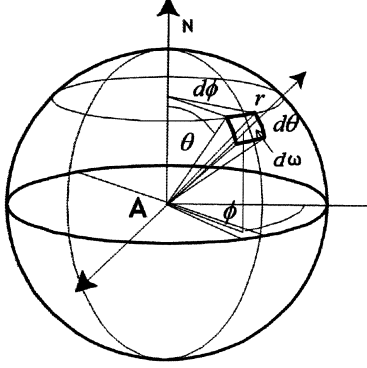


Fig. 1: Calculation of radiance and irradiance value

Consider a point located at the center of the sphere (as shown in Figure 1), then the solid angle  $d\omega$  can be derived from the elevation  $\theta$  and azimuth  $\phi$ :

$$d\omega = \sin \theta d\theta d\phi \quad (1)$$

The energy received by the point  $A$  from a particular direction, surrounded by an infinitesimal solid angle  $d\omega$ , is described as:

$$L(\lambda, \theta, \phi) \cos \theta \sin \theta d\theta d\phi \quad (2)$$

where  $L(\lambda, \theta, \phi)$  is the incident radiance distribution of illumination.

The irradiance value of the point  $A$  can be expressed as the integral of incident energy over the hemisphere whose north pole is at the surface normal direction:

$$E^A = \int_{-\pi}^{\pi} \int_0^{\frac{\pi}{2}} L(\lambda, \theta, \phi) \cos \theta \sin \theta d\theta d\phi \quad (3)$$

In this paper, we assume that the object surface is Lambertian surface, and therefore the reflected light is isotropic. Then, the radiance value of the point  $A$  is expressed as the multiplication of irradiance value  $E$  and reflectance  $S^A$ :

$$I^A = \int_{-\pi}^{\pi} \int_0^{\frac{\pi}{2}} S^A L(\lambda, \theta, \phi) \cos \theta \sin \theta d\theta d\phi \quad (4)$$

### 3 Interreflection Model

If we simply divide the radiance value of a concave object by the irradiance value to acquire the reflectance, the result tends to be brighter than the true value, because of the presence of interreflection. In order to estimate an accurate reflectance, we include the interreflection in our method.

When the surface of a concave object is illuminated, its facets receive light from both light source and other

facets, as shown in Figure 2. In Figure 2, the small facet  $x$  receives light from both light source and another facet  $x'$  on the surface. Therefore, the radiance value at each surface facet has two components, one resulting from the light source and the second due to illumination by other facets. The latter component is called interreflection effect.

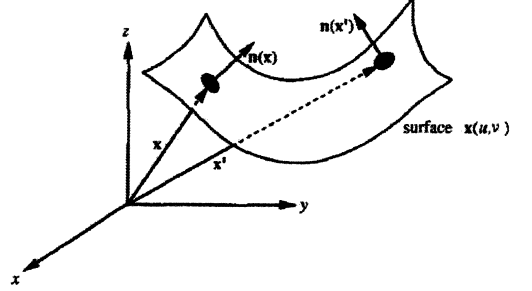


Fig. 2: A concave surface in three-dimensional space [3].

**Radiance due to other facets** The interreflection effect between two facets  $i$  and  $j$  is strongly affected by whether these two facets can see each other or not. The visibility  $V$  between two facets  $i$  and  $j$  is determined by the following function:

$$V_{ij} = \frac{n \cdot (-r) + |n \cdot (-r)|}{2|n \cdot (-r)|} \cdot \frac{n' \cdot r + |n' \cdot r|}{2|n' \cdot r|} \cdot Occ \quad (5)$$

where  $n$  and  $n'$  are unit surface normals of the  $i$ th and  $j$ th facets,  $r$  is the vector from  $j$ th to  $i$ th facet, and  $Occ$  is the coefficient for occlusion between these two facets. If the  $i$ th and  $j$ th facets are occluded by another facet, these two facets can not see each other.

The occlusion coefficient is important to calculate the visibility function. A typical situation when occlusion happens is shown in Figure 3. In Figure 3, the  $i$ th facet lies on the horizontal top plane, while the  $j$ th facet lies on the vertical plane between them, they cannot see each other and there is no interreflection effect between  $i$ th and  $j$ th facets. The occlusion coefficient is calculated as follows: for the vector between the  $i$ th and  $j$ th facets, we detect whether this vector intersects with another facet or not. If the vector intersects with at least one of the other facets, the occlusion coefficient is equal to zero. If not, there is no occlusion between the  $i$ th and  $j$ th facets and the occlusion coefficient is set to one.

The visibility function  $V_{ij}$  in Equation (5) can only have two values, 1 or 0. If it is equal to 1, the  $i$ th and  $j$ th facets see each other and the interreflection between these two facets will be calculated. If not, no interreflection exists between the facets.

Let  $E_{ij}$  be the irradiance value of  $i$ th facet due to the radiance value of the  $j$ th facet  $L_j$ .  $E_{ij}$  can be derived from the definitions of radiance and irradiance (see appendix) and geometry shown in Figure 4:

$$E_{ij} = \left[ \frac{[n \cdot (-r)][n' \cdot r]V_{ij}}{[r \cdot r]^2} \right] L_j S_i \quad (6)$$

where  $S_i$  is the area of the  $i$ th facet,  $V_{ij}$  is the visibility function between the  $i$ th and  $j$ th facets, and  $L_j$  is the radiance value of the  $j$ th facet.

The radiance value  $L_{ij}$  of the  $i$ th facet can be determined from its irradiance value  $E_{ij}$  as:

$$L_{ij} = \frac{\rho_i}{\pi} E_{ij} \quad (7)$$

where  $\rho_i$  is the reflectance of the  $i$ th facet. The reflectance is assumed to be invariable among a facet, since a facet size is sufficiently small. The factor  $\frac{\rho_i}{\pi}$  is the bi-directional reflectance distribution function (see appendix) for a Lambertian surface. From Equations (6) and (7), we obtain

$$L_{ij} = \frac{\rho_i}{\pi} K_{ij} L_j \quad (8)$$

where

$$K_{ij} = \left[ \frac{[n \cdot (-r)][n' \cdot r]V_{ij}}{[r \cdot r]^2} \right] S_i \quad (9)$$

$K_{ij}$  is a coefficient determined by the positions and orientations of the  $i$ th and  $j$ th facet.

From Equation (8), we obtain the radiance value  $L_{ij}$  of  $i$ th facet due to the radiance value of  $j$ th facet, and as described before, this radiance value is the second component of the total radiance value for a small facet lies on the surface of a concave object.

**Radiance due to a light source** The radiance value of the  $i$ th facet directly due to a single point light source (excluding interreflection effect) can be expressed by using the irradiance value:

$$L_{si} = \frac{\rho_i}{\pi} E_{si} \quad (10)$$

where  $E_{si}$  is the irradiance value of the  $i$ th facet directly due to a light source. The irradiance value can be calculated from Equation (3).

**Total radiance** The total radiance value of the  $i$ th facet  $L_i$  can be expressed as a sum of the radiance due to a light source  $L_{si}$  and all the other facets on the surface:

$$L_i = L_{si} + \frac{\rho_i}{\pi} \sum_{j=1}^m L_j K_{ij} \quad (11)$$

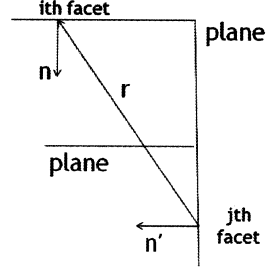


Fig. 3: Occlusion between two facets: the  $i$ th and  $j$ th facets are occluded by the middle horizontal plane

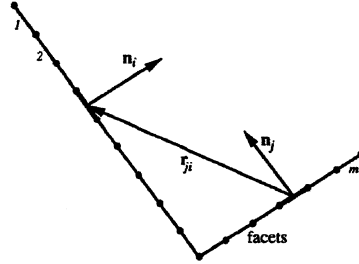


Fig. 4: Modeling the surface as a collection of facets, each with its own radiance and reflectance values [3].

where  $m$  is the number of facets on the object surface. When  $j$  equals to  $i$ , the  $K_{ij}$  coefficient between the  $i$ th and  $j$ th facets becomes zero, according to Equation (9).

The interreflection equation for a concave surface can be written as follows using a vector notation. Let us define the facet radiance vector as  $L = [L_1, L_2, \dots, L_m]^T$ , the source contribution vector as  $L_s = [L_{s1}, L_{s2}, \dots, L_{sm}]^T$ , and the reflectance matrix  $P$  and the  $K_{ij}$  coefficient matrix  $K$  as:

$$P = \frac{1}{\pi} \begin{bmatrix} \rho_1 & 0 & \dots & 0 \\ 0 & \rho_2 & \dots & 0 \\ \dots & \dots & \dots & \dots \\ \dots & \dots & \dots & \dots \\ 0 & 0 & \dots & \rho_m \end{bmatrix} \quad (12)$$

$$K = \begin{bmatrix} 0 & k_{12} & \dots & \dots & \dots \\ k_{21} & 0 & \dots & \dots & \dots \\ \dots & \dots & 0 & \dots & \dots \\ \dots & \dots & \dots & 0 & \dots \\ \dots & \dots & \dots & \dots & 0 \end{bmatrix} \quad (13)$$

Now, the Equation (11) can be written as:

$$L = L_s + PKL \quad (14)$$

The reflectance matrix  $P$  can be derived from Equation (14) as:

$$P = (L - L_s)L^{-1}K^{-1} \quad (15)$$

The parameters of matrix  $P$  are the reflectance of each facet, and can be obtained as:

$$\rho_i = \pi L_i (E_{s_i} + L_1 K_{i1} + L_2 K_{i2} + \dots + L_m K_{im})^{-1} \quad (16)$$

where  $\rho_i$  is the reflectance of the  $i$ th facet,  $L_i$  is the radiance value of the  $i$ th facet,  $E_{s_i}$  is the irradiance value due to the light source, and  $K_{ij}$  is a coefficient between the  $i$ th and  $j$ th facets. The irradiance and radiance values can be calculated from Equations (3) and (4), respectively. The  $K$  coefficient is determined by the geometry of two facets on the object surface, and can be derived from the object shape. From Equation (16), we can acquire the reflectance of each facet on the object surface with the presence of interreflection.

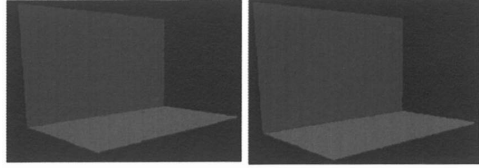
## 4 Experiment

In this section, we will show our experimental results for both simulation and real outdoor objects with the presence of interreflectons. As described before, the interreflection effect on a facet can be calculated as the sum of incoming light energy from all the other facets by assuming that the object surface consists of hundreds of small facets. From the experimental result, we can see the improvement achieved by this method.

### 4.1 Simulation object

First we applied our method to estimate the reflectance of a simulation object. We use the Radiance software [18] to define two planes perpendicular to each other. One and the other plane have the reflectance of (0.1, 0.2, 0.7) and (0.7, 0.1, 0.1) for the three RGB channels, respectively. After rendering using Radiance software, the acquired image is the radiance image of the defined object. This image can be also called as observation, the pixel value of observation is the radiance value of corresponding facets.

The irradiance value of a small facet due to light source ( $E_{s_i}$  in Equation (16)) is proportional to cosine of the angle between the source direction and the surface normal direction of the small facet, that is  $E_{s_i} = kn \cdot s$ . The constant of proportionality  $k$  is determined by the radiant intensity of the source and its distance from the surface. Then, in Equation (16), for each facet, we can read the radiance value from the observation, calculate the irradiance value as the multiplication of constant  $k$  and dot production, also the  $K_{ij}$  coefficient can be calculated from Equation (9).



(a) Observation. (b) Synthesized image.

Fig. 5: (a) Radiance image of simulation object (b) Synthesized image rendering with the estimated reflectance

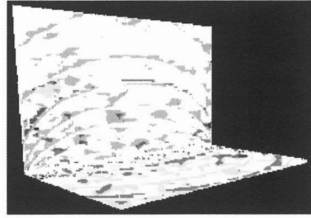


Fig. 6: Difference image (10 times brighter) between observation and synthesized image

Figure 5(a) shows the simulation object. We use the estimated reflectance and the same light condition to re-render the simulation object, and get the synthesized image of this object. This synthesized image is shown in Figure 5(b). Figure 6 shows the difference between the observation and the synthesized image. The difference is less than 4 percent for two planes. This means the pixel value of synthesized image is similar to observation.

### 4.2 Real outdoor object

For the experiment of real outdoor object, we choose the clock tower in Tokyo University campus. Unlike the simulation object, it is much harder to estimate the accurate reflectance of a real outdoor object, because the light source for an outdoor object can not be controlled. For light source of an outdoor object, we used image based lighting to render the object.

**Observation capture and shape acquisition** We used the range sensor Cyrax 2500 [19] to acquire the object shape information. The object shape is shown in Figure 7. We used a spherical motion camera Ladybug2 to capture the radiance value of object surface. The Ladybug2 camera can capture both the radiance value of clock tower and the light condition around the clock tower. The observation is shown in Figure 8.

Figure 7 shows acquired shape of clock tower. From the shape, we can get the surface normal and 3D coordinate of each facet on the object surface. Figure 8 shows the captured image used for both radiance value of each facet

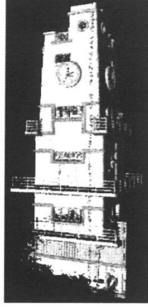


Fig. 7: Acquired shape of clocktower



Fig. 8: Observation of clocktower

and the light source for rendering the clock tower. One advantage of doing this is that the clock tower and light source have the same camera sensitivity, the other is that we do not need the geometrical calibration between the target object image and illumination environment.

**Radiance calculation** In the experiment of clock tower, the radiance value of each facet is read from the radiance image. The radiance image is shown in Figure 9.



Fig. 9: Radiance image of clocktower

**Irradiance calculation** The irradiance value directly due to the light source can be calculated from Equation (3). We used Radiance software to do the irradiance calculation. Specifically, first we set the reflectance of each

facet to be 1.0, then render the clock tower by image based lighting. The image rendered is the irradiance image, shown in Figure 10.

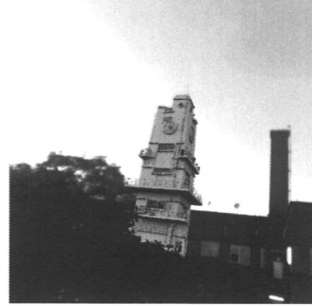
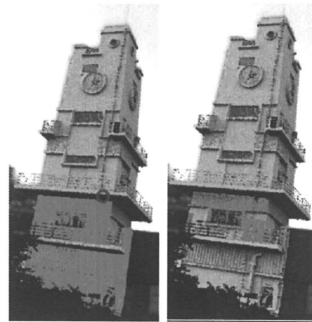


Fig. 10: Irradiance image of clocktower

**Reflectance estimation** Known the surface normal and three dimensional coordinate of each facet from acquired shape, the  $K_{ij}$  coefficient can be calculated from Equation (9). By using the radiance value read from the radiance image of clocktower and irradiance value calculated from Equation (3), we can calculate the reflectance of each facet according to Equation (16).

As shown in Figure 3, even though the visibility function without occlusion coefficient between these two facets is equal to 1, these two facets actually can not see each other because of the occlusion. Figure 11 shows this kind of situation.

When estimating the reflectance of the small facet lies in the blue circle, the  $K_{ij}$  coefficient is calculated between this facet and all the other red facets shown in Figure 11(a). Apparently, there are too many red facets that this facet actually can not see. But the  $K_{ij}$  coefficient was included in the sum as interreflection effect because of the



(a) K coefficient. (b) K coefficient.

Fig. 11: (a)K coefficient calculation with occlusion (b) K coefficient calculation without occlusion

occlusion between them. Without occlusion coefficient, the calculated interreflection effect would be too large, the estimated reflectance would be too small. We solve this occlusion problem by applying the occlusion coefficient to visibility function calculation. Specifically, we detect whether the vector between the  $i$ th and  $j$ th facets intersects with all the other facets or not. If the vector intersects with at least one of the other facets, then the occlusion coefficient is equal to 0, so is the  $K_{ij}$  coefficient. If not, the visibility function is equal to 1, and the  $K_{ij}$  coefficient can be calculated from Equation (9).

Figure 11(b) shows the situation when dealing with the occlusion problem by the method described before. The red facets have the same meaning as Figure 11(a). For the same facet, the number of red facets in Figure 11(b) is only around one third of Figure 11(a). Two thirds of red facets in Figure 11(a) are occluded, and should not be seen by the facet lies in the blue circle. With the occlusion coefficient, the estimated reflectance becomes much more accurate.

Figure 12 shows the estimated reflectance image of clocktower using our method.

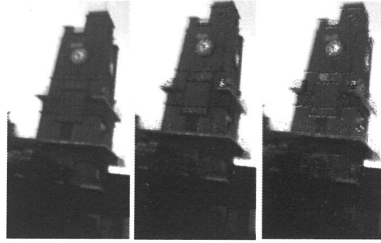


Fig. 12: Reflectance image of clocktower

In order to evaluate the estimated reflectance, we used the image based lighting method to render the clock tower, the result is shown in Figure 13.

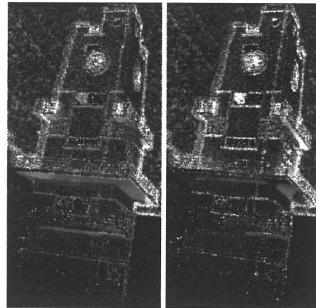
Figure 13(a) is the observation of clock tower, (b) is the result rendered by the previous method, (c) is the result rendered by our method. From Equations (3) and (4), if we divide the radiance value by the irradiance value of each facet, we can get the reflectance of this facet without interreflection effect. Okura et al. [20] use this method to estimate the reflectance of an outdoor object. Figure 13(b) was rendered by this way, there is no interreflection effect for each facet on the object surface. Figure 13(c) shows the synthesized image rendering with estimated reflectance, which are obtained by our method.

Figures 14(a) and (b) show the difference between observation of clock tower (Figure 13(a)) and synthesized image without interreflection (Figure 13(b)) and with in-



(a) Truth value.(b) No interreflection. (c) Interreflection.

Fig. 13: (a) Observation of clocktower (b) Synthesized image without interreflection (c) Synthesized image with estimated reflectance



(a) No interreflection. (b) Interreflection.

Fig. 14: (a) Difference between observation and re-rendered image without interreflection (b) Difference between observation and re-rendered image with interreflection

terreflection (Figure 13(c)), respectively. From the comparison between Figures 14(a) and (b), for most concave parts of clock tower, if including the interreflection effect, the synthesized looks much more realistic. The difference between the synthesized image with interreflection and radiance image of clock tower, especially for the concave parts, is less than three percent. But for synthesized image without interreflection, the difference is bigger than sixty percent.

In the synthesized image rendered with estimated reflectance by our method (Figure 13(c)), there are still some parts which have large errors. We consider that these errors might be caused by lack of whole geometry and calibration error between 3D object and 2D image.

## 5 Conclusion

In this paper, we have proposed a new method to estimate the accurate reflectance of object surface with the presence of interreflection by assuming that the object surface consists of hundreds of small facets, and the in-

terreflection effect of one small facet is calculated as the sum of incident energy of all the other facets. This technique takes shape and observation as input to estimate the reflectance of object surface. Then, the estimated reflectance can be used for synthesizing image of the object. We also solve the problem caused by occlusion between two facets, the occlusion can affect the estimated reflectance so much that it makes the synthesized image appear very dark. The experiment result shows that the synthesized image rendering with estimated reflectance is very similar to observation.

## A Appendix: Radiometric Definitions

Definitions of radiometric terms which are used in the analysis of interreflection are described as follows (detailed derivations of these terms are given by Nicodemus et al. [21]). Figure 14 shows a surface element illuminated by a source of light. The irradiance  $E$  of the surface is defined as the incident flux density ( $W/m^2$ ):

$$E = \frac{d\Phi_i}{dA} \quad (17)$$

where  $d\Phi_i$  is the flux incident on the area  $dA$  of the surface facet. The radiance  $L$  of the surface is defined as the flux emitted per unit foreshortened area per unit solid angle ( $W/m^2/sr$ ). The surface radiance in the direction  $(\theta_r, \phi_r)$  is determined as

$$L = \frac{d^2\Phi_r}{dA \cos\theta_r d\omega_r} \quad (18)$$

where  $d^2\Phi_r$  is the flux radiated within the solid angle  $d\omega_r$ . The Bidirectional Reflectance Distribution Function (BRDF) of a surface is a measure of how bright the surface appears when viewed from one direction while it is illuminated from another direction. The BRDF is described as:

$$f = \frac{L}{E} \quad (19)$$

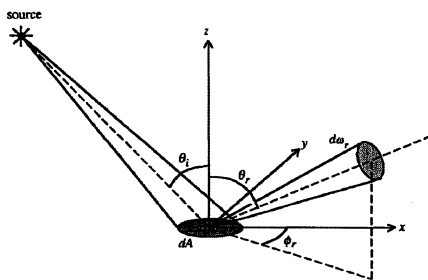


Fig. 15: Geometry used to define radiometric terms [3].

## References

- [1] K.Ikeuchi, and D.Miyazai, "Digitally Archiving Cultural Objects," Springer science Business Media, LLC, 2008
- [2] K. Ikeuchi, T. Oishi, J. Takamatsu, R. Sagawa, A. Nakazawa, R. Kurazume, K. Nishino, M. Kamakura, and Y. Okamoto, "The great buddha project: Digitally archiving, restoring, and analyzing cultural heritage objects," *Intl J.Com.* V.75-1, pp.189-208, 2007
- [3] S.K.Nayar, K.Ikeuchi, and T.Kanade, "Shape from Interreflections," *International Journal of Computer Vision*, 6:3, 173-195, 1991
- [4] Y.Yu, P.Debevec, J.Malik, and T.Hawkins, "Inverse Global Illumination: Recovering Reflectance Models of Real Scenes from photographs," *SIGGRAPH*, 1999
- [5] K.Pulli, M.Cohen, T.Duchamp, H.Hopper, L.Shapiro and W.Stuetzle, "View-based rendering: Visualizing real objects from scanned range and color data," in *Proc.EUROGRSPHICS Workshop*, pp.23-34, 1997
- [6] P.J.Neugebauer, and K.Klein, "Texturing 3D models of real world objects from multiple unregistered photographic views," *Computer Graphics Forum* pp. 18-3, 245-256, 1999
- [7] H.P.A.Lensch, W.Heidrich, and H.P.Seidel, "Automated texture registration and stitching for real world models," *Pacific Graphics*, pp.317-326, 2000
- [8] L.Wang, S.B.Kang, R.Szeliski and H.Y.Shum, "Optimal texture map reconstruction from multiple views," in *Proc.CVPR*, pp.347-354, 2001
- [9] F.Bernardini, I.M.Martin and H.Rushmeier, "High-quality texture reconstruction from multiple scans," *IEEE Trans. Vis. Comput. Graph.* 7-4, pp.318-332, 2001
- [10] K.J.Dana, B.van Ginneken, S.K.Nayer, and J.J. Koenderink, "Reflectance and texture of real-world surfaces," *CVPR*, pp.151-157, 1997
- [11] S.Lin and S.W.Lee, "Estimation of diffuse and specular appearance," in *Proc.ICCV*, pp.855-860, 1999
- [12] T.Machida, N.Yokoya and H.Takemura, "Surface reflectance modeling of real objects with interreflections," in *Proc.ICCV*, pp.170-177, 2003
- [13] I.sato, T.Okabe, Y.sato and K.Ikeuchi, "Appearance sampling for obtaining a set of basis images for variable illumination," in *Proc.ICCV*, pp.800-807, 2003
- [14] H.Winnemoller, A.Mohan, J.Tumblin, and B.Gooch, "Light waving:Estimating light positions from photographs alone," *Computer Graphics Forum* 24-3, 433-438, 2005
- [15] Y.Sato, M.D.Wheeler, and K.Ikeuchi, "Object Shape and Reflectance Modeling from Observation," *SIGGRAPH*, pp.379-387, 1997
- [16] S.K.Nayar, G.Krishnan, M.Grossberg, and R.Raskar, "Fast Separation of Direct and Global Components of a Scene using High Frequency Illumination," *SIG-*

GRAPH, pp.935-944, 2006

- [17] Y.Weiss, "Deriving intrinsic images from image sequences," ICCV, pp.68-75, Volume 2, 2001
- [18] <http://radsite.lbl.gov/radiance/>
- [19] <http://www.meab-mx.se/tidning/cyrax2500.htm>
- [20] S.Okura, R.Kawakami, and K.Ikeuchi, "Efficient Estimation of Diffuse Surface Reflectance in an Outdoor Scene using Spherical Images," MIRU, 2008
- [21] Nicodemus, F.E., Richmond, J.C., Hsia, J.J., Ginsberg, I.W., and Limperis, T., "Geometrical considerations and nomenclature of reflectance," NBS Monograph 160, National Bureau of Standards, October, 1977